

# Pressure, Temperature, and Composition Dependence of Deuterium Spin-Lattice Relaxation Times in Undercooled $\text{MgCl}_2/\text{D}_2\text{O}$ Solutions

W. Fink and E. W. Lang\*

*Institute of Biophysics and Physical Biochemistry, University of Regensburg,  
POB 397, D-8400 Regensburg, FRG (Received: January 6, 1988; In Final Form: April 6, 1988)*

Nuclear magnetic relaxation time measurements are well suited to monitor orientational and positional fluctuations of water molecules in liquids. Hence the dependence of deuterium spin-lattice relaxation rates on pressure, temperature, and composition are reported in  $\text{MgCl}_2/\text{D}_2\text{O}$  solutions over wide ranges of the external variables. The anomalous increase of molecular mobility upon compression, observed in neat undercooled water, becomes less pronounced with increasing salt concentration until the effect vanishes at the edge of the glass-forming composition range. Under high hydrostatic pressure or high solute concentration, orientational fluctuations of water molecules show characteristics which resemble those of configurational fluctuations of liquids approaching their respective glass transition. Conclusions are drawn regarding the influence of structure and composition on molecular motions, and details of orientational fluctuations of water molecules coordinated to  $\text{Mg}^{2+}$  ions are deduced within a motional model proposed recently, which is consistent with the local structure in these solutions.

## Introduction

The diffusive modes of molecular motions in aqueous solutions result from orientational and positional fluctuations. Their time dependence may be characterized by appropriate correlation functions  $G(t)$  of the fluctuating orientational and/or spatial variables. Nuclear magnetic relaxation rates  $R_1 = 1/T_1$  are proportional to the spectral density function  $g(\omega) \approx \int G(t) \exp(i\omega t) dt$  of these fluctuations.<sup>1</sup> Under ambient conditions the latter are fast (picoseconds) on the time scale of the NMR experiment (nanoseconds). This renders the information about the molecular dynamics limited to an average correlation time  $\tau_{av}$

$$R_1 = 1/T_1 \approx g(\omega=0) \approx \int G(t) dt \approx G(0)\tau_{av} \quad (1)$$

of the relevant fluctuations. Furthermore  $\tau_{av}$ , the inverse of which may be taken as a rough measure of molecular mobility, cannot be separated easily from the structural information contained in  $G(0)$ . However, upon addition of network-breaking agents like salt or hydrostatic pressure, aqueous emulsions can be undercooled to increasingly lower temperatures. This is because the low-temperature limit is set by the homogeneous nucleation temperature  $T_H$ , which is a strongly decreasing function of pressure and/or solute concentration.<sup>2</sup> Eventually nucleation may become kinetically impossible; hence the solutions freeze to an amorphous solid at the glass transition temperature  $T_g$ .<sup>3</sup> Upon cooling, molecular motions in aqueous solutions slow down strongly and the spin-lattice relaxation rates increase.<sup>4</sup> At low temperatures a maximum rate can be observed. This is generally the case in aqueous emulsions under high hydrostatic pressure ( $p \approx 200$  MPa).<sup>5</sup> At lower pressure ( $p \leq 200$  MPa) it may be observed in highly concentrated electrolyte solutions only.<sup>6</sup> In this slow-motion regime the relaxation rates become sensitive to the form of the spectral density function. Thus more detailed information about orientational and/or positional fluctuations may possibly be gathered. Also parameters may be deduced characterizing the average local structure in the solutions.

In this investigation deuterium ( $^2\text{H}$ ) spin-lattice relaxation times are reported in undercooled  $\text{MgCl}_2/\text{D}_2\text{O}$  solutions in the concentration range  $0.1 \text{ m} < c < 5 \text{ m}$ . The temperature was varied between room temperature and the respective homogeneous nucleation temperature  $T_H(c,p)$  and the pressure was raised to 225 MPa.

## Experiment

To prevent heterogeneous nucleation upon cooling, all salt solutions had to be prepared as emulsions. Prior to use the six  $\text{H}_2\text{O}$  molecules of the hexahydrate  $\text{MgCl}_2 \cdot 6\text{H}_2\text{O}$  (Merck,

Darmstadt, FRG) had to be replaced by  $\text{D}_2\text{O}$  quantitatively. The hexahydrate was dissolved in distilled  $\text{D}_2\text{O}$ , dried under vacuum at 313 K, and stored over  $\text{P}_2\text{O}_5$  on a vacuum line for 48 h. After this procedure was repeated four times, the desired concentration was prepared from a stock solution by adding the proper amount of heavy water. Emulsions were prepared by mixing equal amounts of the salt solution with a mixture of methylcyclohexane (24 wt %), methylcyclopentane (24 wt %), and the surfactant sorbitan tristearate (2 wt %). Before mixing, all components had to be degassed by at least five freeze-pump-thaw cycles to remove dissolved oxygen. The mixing was done in a glovebox under an argon atmosphere by pressing the mixture through a stainless steel net within a syringe. Finally the emulsion had to be filled in the strengthened high-pressure glass cell<sup>7</sup> on a vacuum line. All  $T_1$  experiments were performed with the inversion recovery pulse sequence (Freeman-Hill modification) on a Varian XL-100 spectrometer at 15.35 MHz. The 225-MPa isobars of the 3 and 5 m solutions could be measured on a Bruker MSL 300 spectrometer at 46.07 MHz also. The relaxation times are considered reliable to  $\pm 10\%$ . The temperatures were measured with a miniature chromel-alumel thermocouple (Philips, Kassel, FRG) and are accurate to  $\pm 1$  K. The pressure was measured with a precision Bourdon gauge (Heise, CT) to  $\pm 0.5$  MPa.

## Theory

*The Motional Model for Hydration Water.* A quantitative discussion of the dynamics of the water molecules in these solutions can be given in terms of a motional model developed recently to deduce the form of the spectral density function  $g(\omega)$  for water molecules adjacent to a strongly hydrating cation.<sup>5,6,8,9</sup> The model decomposes the orientational fluctuations of the water molecules into small-amplitude librations about their mean orientation (see Figure 1). These fast torsional oscillations are superimposed onto

(1) Volino, F. In *Microscopic Structure and Dynamics of Liquids*; Dupuy, J., Dianoux, A. J., Eds.; Plenum: New York, 1978; Chapter 3.

(2) Angell, C. A. In *Water-A Comprehensive Treatise*; Franks, F., Ed.; Plenum: New York, 1982; Vol. 7, Chapter 1.

(3) Angell, C. A.; Tucker, J. C. *J. Phys. Chem.* **1980**, *84*, 268.

(4) Lang, E. W.; Lüdemann, H.-D. *Angew. Chem., Int. Ed. Engl.* **1982**, *21*, 315.

(5) Lang, E. W.; Piculell, L. In *Water and Aqueous Solutions*; Neilson, G. W., Enderby, J. E., Eds.; Hilger: Bristol, U.K., 1986; p 31.

(6) Lang, E. W.; Lüdemann, H.-D. *Ber. Bunsen-Ges. Phys. Chem.* **1985**, *89*, 508.

(7) Lang, E. W.; Rauchschwalbe, R.; Lüdemann, H.-D. *High Temp.-High Press.* **1977**, *9*, 519.

(8) Lang, E. W.; Prielmeier, F. X. *Ber. Bunsen-Ges. Phys. Chem.* **1988**, *92*, 717.

(9) Lang, E. W.; Radkowsch, H.; Fink, W. *Proc. XI AIRAPT Conf., Kiev, 1987*, in press.

\* To whom all correspondence concerning this article should be addressed.

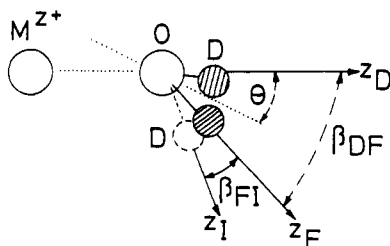


**Figure 1.** Illustration of the local structure of the cation-water arrangement with the various coordinate frames involved in the motional model.

anisotropic fluctuations around the local director with correlation time  $\tau_i$ . It may be expected that fluctuations around the director are less strongly hindered than fluctuations about any other axis perpendicular to the director.<sup>10</sup> To keep the model simple with a minimum of adjustable parameters only these least hindered fluctuations around the local director are taken into account. In addition to these internal modes there is an isotropic tumbling of the hydration complex or an uncorrelated isotropic diffusion of the molecules around the ion with correlation time  $\tau_r$ . At least for second-shell water molecules chemical exchange between hydration sites and bulk sites must be accounted for, because the mean residence time of these water molecules,  $\tau_{\text{ex}}$ , is comparable with the average correlation time.<sup>11</sup>

**The Relaxation Rate of Hydration Water.** The model yields the following expression for the deuteron relaxation rate of the hydration water<sup>6</sup>

$$(R_1)_{\text{hyd}} = (3\pi^2/20)((\chi_{\text{eff}})^2/\omega_0)((1/4)(3 \cos^2 \beta_{\text{DF}} - 1)^2 F(\omega_0\tau_0) + 3 \sin^2 \beta_{\text{DF}} \cos^2 \beta_{\text{DF}} F(\omega_0\tau_1) + (3/4) \sin^4 \beta_{\text{DF}} F(\omega_0\tau_2)) \quad (2)$$

with the quadrupole coupling constant  $\chi$ , averaged over the librations, given by

$$\chi_{\text{eff}} = (\sum |\langle D_{02}^2(\Omega_{\text{FI}}) \rangle|^2)^{1/2} \chi \quad (2a)$$

$$\simeq (1/2)(3(\cos^2 \beta_{\text{FI}}) - 1)\chi$$

$\beta_{\text{FI}}$  is the angle between the  $z$  axis of the instantaneous principal frame of the electric field gradient tensor (I) and the equilibrium orientation of the OD bond (F) in the quasi-static local configuration (see Figure 1).  $\beta_{\text{DF}}$  relates this equilibrium orientation of the OD bond to the local director frame (D). Furthermore

$$F(\omega\tau) = 2g(\omega\tau) + 8g(2\omega\tau) \quad (3)$$

$$g(m\omega\tau) = \omega\tau/(1 + (m\omega\tau)^2) \quad (3a)$$

and

$$1/\tau_0 = 1/\tau_r + 1/\tau_{\text{ex}} \quad (3b)$$

$$1/\tau_1 = 1/\tau_0 + 1/\tau_i \quad (3c)$$

$$1/\tau_2 = 1/\tau_0 + 4/\tau_i \quad (3d)$$

**Main Assumptions.** These expressions imply that time-scale separation pertains between the torsional and the diffusive modes, that the anisotropic diffusive mode with correlation time  $\tau_i$  and the isotropic overall tumbling mode with correlation time  $\tau_r$  are statistically independent, that the mean residence time  $\tau_{\text{ex}}$  for second-shell water molecules is at least of the order of the correlation times ( $\tau_{\text{ex}}$  may be neglected for the water molecules of the hexaquo complex), and that the interaction is completely randomized on exchange.<sup>12</sup> This is a reasonable assumption for small ions or molecules because of the vanishingly small probability for surface reencounters within  $\tau_r$ . Further an exponential decay

of the orientational correlation functions for times  $t > \tau_r$  is implied by eq 3a, though nonexponential correlation functions are often observed in undercooled systems.

**The Temperature Dependence of the Correlation Times.** A characteristic feature of average structural relaxation times in undercooled, glass-forming systems is their strong non-Arrhenius temperature dependence. It is a consequence of collective fluctuations and can be accommodated often by a VTF law,<sup>13-15</sup> which represents the  $T$  dependence of dynamic properties in most dense liquids above their glass transition rather well. Within the current two-mode approximation the  $T$  dependence of overall tumbling and exchange processes will therefore be represented by

$$\tau_0 = \tau_{00} \exp(B_T/(T - T_0)) \quad (4)$$

with  $T_0$  the temperature of global motional arrest. It corresponds to calorimetric glass transitions in the limit of small cooling rates.

The anisotropic fluctuations around the local director clearly correspond to a thermally activated crossing over barriers. Hence their  $T$  dependence should be given by an Arrhenius law

$$\tau_i = \tau_{i0} \exp(E_a/(kT)) \quad (5)$$

with the preexponential factor corresponding to an attempt frequency for barrier crossing; i.e., it is the inverse of an average librational frequency.

**The Two-Site Approximation.** The above expressions pertain to the relaxation rate of water molecules at cationic hydration sites. Because the exchange between hydration sites and bulk sites is fast ( $T_1 > \tau_{\text{ex}}$ ), in more dilute solutions an average relaxation time can be observed only. It may be calculated within a two-site approximation<sup>6</sup> as a mole fraction weighted average according to

$$R_1(T, p, R) = (n_h/R)(R_1)_{\text{hyd}} + ((R - n_h)/R)(R_1)_{\text{bulk}} \quad (6)$$

Orientalional fluctuations in the bulk phase are assumed to be isotropic despite the presence of the anions. This is reasonable in view of the weak anion-water interactions and the short mean residence time of water near anions. The bulk rate is given by an expression similar to pure compressed  $\text{D}_2\text{O}$ .<sup>5,16</sup> (Note that, in our notation, bulk water differs from pure water because of the presence of the anions. The latter certainly impose geometrical constraints upon the orientation of adjacent waters but do not alter their dynamics appreciably on the time scale of relevance.)

## Results

**Effects of Pressure and Ionic Solutes.** The isothermal pressure dependence of the  $^2\text{H}$   $T_1$  is shown in Figure 2 for various concentrations. In the undercooled phase  $T_1$ , hence the average rotational mobility of the water molecules, increases upon compression. The effect is most pronounced at low temperatures and low concentrations. For concentrations  $c \geq 3$  *m*, corresponding to the glass-forming composition range  $R \geq 18$  ( $R$  = moles of  $\text{D}_2\text{O}$ /mole of salt),  $T_1$  is independent of pressure ( $p \leq 225$  MPa).

Addition of ionic solutes also give shorter relaxation times,  $T_1$ , which means a slowing down of orientational fluctuations (see eq 1) at ambient temperature (see Figure 3). In the undercooled phase a quite different pattern emerges. At ambient pressure  $T_1$  increases upon addition of solutes, reaches a maximum at  $c \approx 1$  *m* and decreases at still higher concentrations. However, because  $T_1$  in neat  $\text{D}_2\text{O}$  increases much stronger with pressure than in any of the solutions, at high pressure the normal decrease of  $T_1$  with increasing solute concentration is observed. A strikingly similar behavior is found in  $\text{LiCl}/\text{D}_2\text{O}$  solutions, if all concentrations in the latter system are scaled by a factor of 3 roughly (see Figure 3).

**Relaxation Rate Maximum and the Glass Transition.** Figure 4 shows the high-pressure ( $p = 225$  MPa) isobars for all the

(10) Szasz, Gy. I.; Dietz, W.; Heinzinger, K.; Palinkas, G.; Radnai, T. *Chem. Phys. Lett.* **1982**, 92, 388.

(11) Hewish, N. A.; Enderby, J. E.; Howells, W. S. *J. Phys. C: Solid State Phys.* **1983**, 16, 1777.

(12) Wennerström, H. *Mol. Phys.* **1972**, 24, 69.

(13) Vogel, H. *Phys. Z.* **1921**, 22, 645.

(14) Tammann, G.; Hesse, W. Z. *Anorg. Chem.* **1926**, 156, 245.

(15) Fulcher, G. S. *J. Am. Ceram. Soc.* **1925**, 77, 3701.

(16) Lang, E. W.; Lüdemann, H.-D.; Piculell, L. *J. Chem. Phys.* **1984**, 81, 3820.

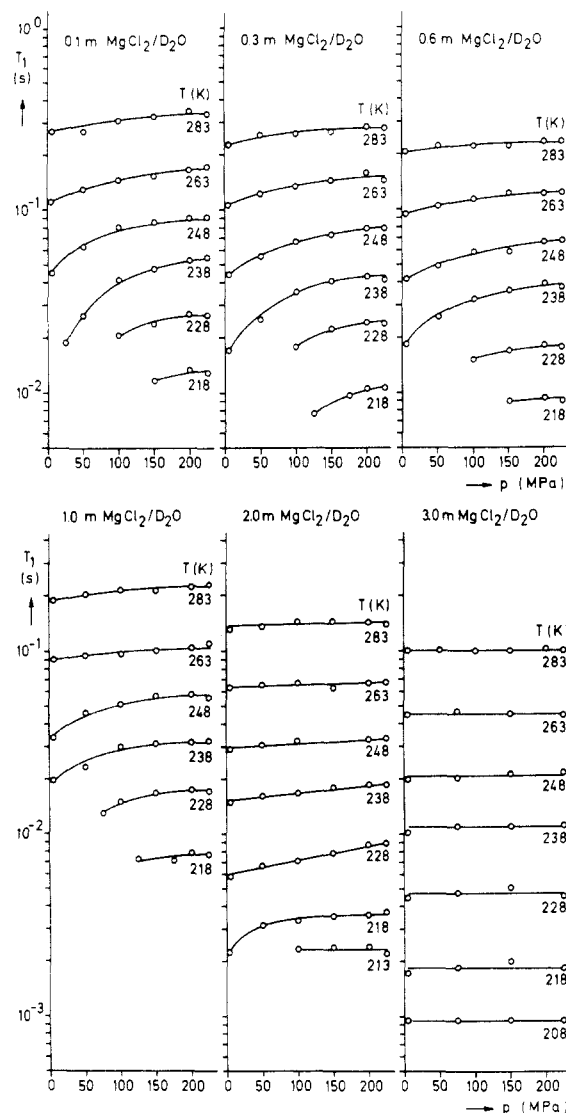


Figure 2. Isothermal pressure dependence of deuteron spin-lattice relaxation times  $T_1$  at various concentrations  $c$  ( $c$ , moles of salt/kg of  $D_2O$ ).

solutions investigated. The data extend to the lowest temperatures where  $T_1$  could be measured. At still lower temperatures the spectral lines became very broad, characteristic of a solid. All the isobars exhibit a  $T_1$  minimum. At temperatures near and below the  $T_1$  minimum the spin-lattice interaction fluctuates at a rate comparable with the Larmor period  $2\pi/\omega_0$ . Hence the  $T_1(T)$  curves become frequency dependent in this slow-motion regime. The temperatures  $T_{\min}$  of the  $T_1$  minimum shift to higher temperatures with increasing solute concentration. In the glass-forming composition range the minimum temperature  $T_{\min}$  of the  $T_1(T)$  isobars (but note  $T_1 \neq f(p)$ ) shows a concentration dependence similar to the calorimetric glass-transition temperature  $T_g$  (see Figure 5). This empirical correlation indicates that the slow-motion regime ( $\omega\tau \approx 1$  in eq 3a) is reached in these solutions of composition  $R \geq 16$  at a comparable distance ( $T_{\min} - T_g$ ) from the respective glass transition. It immediately suggests that all dynamic properties should be compared at equal reduced temperatures ( $T - T_g$ ), since the influence of ionic solutes upon the dynamics of water molecules in these solutions seems to be determined largely by their effect on  $T_g$ . This observation lends strong support to the VTF law (eq 4).

#### Data Analysis

**Model Parameters and Hydration Water Relaxation Rate ( $R_1$ )<sub>hyd</sub>.** From the high-pressure isobars all pertinent parameters of the motional model for the hydration water relaxation rate (eq 2) may be deduced. These isobars extend well into the slow-motion regime (especially the high-field data) where the relaxation time

TABLE I: Glass Temperature  $T_0$  (K) As Predicted from Observed Temperatures  $T_{\min}$  (K) of Minimal  $T_1$  for All Compositions  $R$  (moles of  $D_2O$ /mole of Salt) Investigated

$R$	499	166	83	50	25	16.7	12.5	10
$T_{\min}^a$	192	192	194	195	199	203	213	218
$T_{\min}^b$						211		225
$T_0$	132	132	134	135	138	144	152	160

<sup>a</sup>  $\omega/2\pi = 15.35$  MHz. <sup>b</sup>  $\omega/2\pi = 46.07$  MHz.

curves become sensitive to the details of molecular motions. The 3 m solution may be viewed as containing only water molecules which belong to the first and second hydration shell of the  $Mg^{2+}$  cations. Hence those parameters that could not be obtained from independent sources have been estimated from the high-field  $T_1$  data of the 3 m solution. (Note that they are averages over both hydration shells.)

**1. Structural Parameters.** MD simulations<sup>17-19</sup> and X-ray scattering data<sup>19-21</sup> yield information on the local structure of the cationic hydration shells. The six innermost water molecules are highly ordered with an average tilt angle ( $\Theta$ ) of  $20^\circ$  (see Figure 2).<sup>18</sup> Even the 12 next nearest neighbors are as strongly oriented as the hydration water of  $Na^+$  with a mean tilt angle ( $\Theta$ )  $\approx 52^\circ$ .<sup>18</sup> The angle  $\beta_{DF}$  (see Figure 1), calculated from the tilt angle, does not differ much between a trigonal and a tetragonal orientation, so the latter has been assumed for simplicity.<sup>8</sup> The small variation of  $\beta_{DF}$  implies that  $^2H$   $T_1$  data are not very sensitive to the orientation of the hydration water molecules within the range of tilt angles found from diffraction experiments or computer simulations.

The librally averaged quadrupolar coupling constant  $\chi_{\text{eff}}$  can be estimated reliably from the observed rate maximum  $1/T_1$  ( $T_{\min}$ ). As a matter of fact, the local anisotropic mode does not influence significantly the maximal rate calculated.  $\chi_{\text{eff}}$  is found to be reduced by  $\approx 5\%$  relative to neat  $D_2O$  under comparable conditions. A decreasing  $\chi(^2H)$  reflects an increasing OD bond length for hydration water molecules.<sup>22,23</sup>

**2. Dynamic Parameters.** Except for these structural parameters the shape of the relaxation time curve  $T_1(T)$  strongly depends on the  $T$  dependence of the relevant correlation times (eq 4a and 4b).

To estimate the temperature of global motional arrest  $T_0$  for a solution of composition  $R$  (VTF law, eq 4a) the aforementioned empirical correlation between  $T_g(R, p = 0.1$  MPa) and  $T_{\min}(R, p = 225$  MPa) has been extended to correlate  $T_0(R)$  with  $T_{\min}(R)$ . We further assume that this correlation holds for all compositions, even those outside the glass-forming composition range ( $R \geq 18$ ).  $T_{\min}(R, p = 225$  MPa) and  $T_0(R = \infty, p = 225$  MPa) =  $132$  K<sup>16</sup> can then be used to predict  $T_0(R)$  compiled in Table I.

Taking the abovementioned correlation for granted, a modified Arrhenius diagram,  $\ln T_1$  versus  $(T - T_0)^{-1}$ , reveals that the slope parameter  $B_r$  is identical with that of neat  $D_2O$ <sup>16</sup> under high pressure and is independent of concentration as has been observed in aqueous LiCl solutions also.<sup>5,6</sup> The preexponential factor  $\tau_{00}$  can easily be calculated from data at high temperatures once  $\chi_{\text{eff}}$  has been fixed, because the local anisotropic mode does not contribute to the relaxation significantly in the fast-motion regime.

The preexponential factor  $\tau_{10}$  of the Arrhenius law (eq 5) is identified with the inverse of an average frequency of librations. The latter are hardly investigated for hydration water of divalent cations.<sup>24,25</sup> An average librational frequency of  $500$  cm<sup>-1</sup>,

(17) Heinzinger, K. *Physica B (Amsterdam)* **1985**, *131B*, 196.

(18) Dietz, W.; Riede, W. O.; Heinzinger, K. *Z. Naturforsch.* **1982**, *37a*, 1038.

(19) Palinkas, G.; Radnai, T.; Dietz, W.; Szasz, Gy. I.; Heinzinger, K. *Z. Naturforsch.* **1982**, *37a*, 1049.

(20) Caminiti, R.; Licheri, G.; Paschina, G.; Piccaluga, G.; Pinna, G. *Z. Naturforsch.* **1980**, *35a*, 1361.

(21) Skipper, N. T.; Cummings, S.; Neilson, G. W.; Enderby, J. E. *Nature* **1986**, *321*, 52.

(22) Cummins, P.; Bacskey, G. B.; Hush, N. S.; Engström, S.; Halle, B. *J. Chem. Phys.* **1985**, *82*, 2002.

(23) Mayas, L.; Plato, M.; Winscom, C. J.; Möbius, K. *Mol. Phys.* **1978**, *36*, 753.

(24) Safford, G. J.; Leung, P. S.; Naumann, A. W.; Schaffer, P. C. *J. Chem. Phys.* **1969**, *50*, 4444.

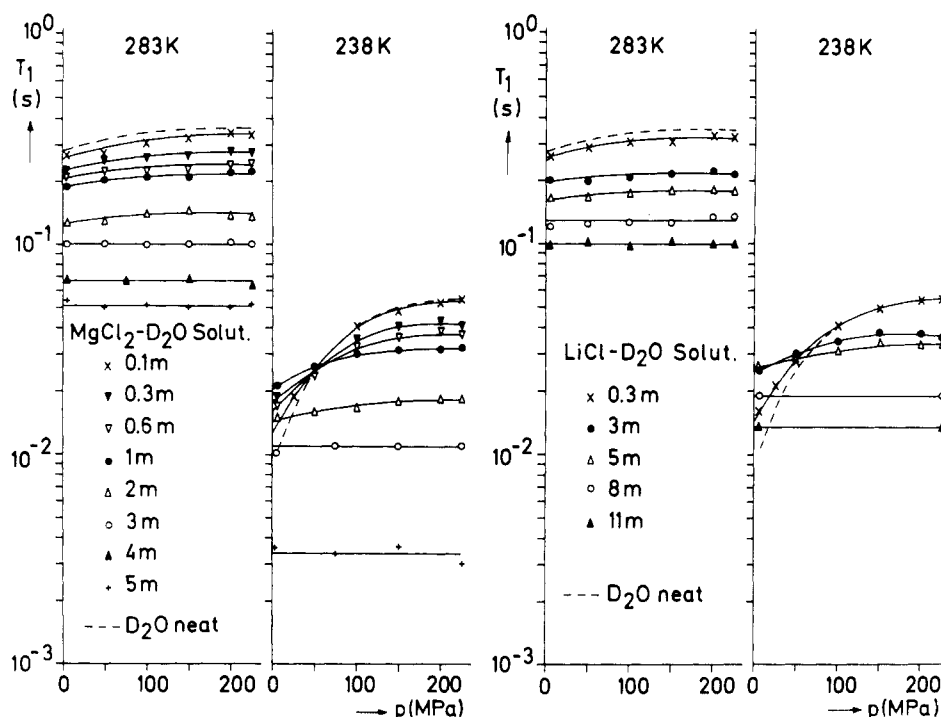


Figure 3. Comparison of  $T_1(^2\text{H})$  isotherms at various concentrations  $c$  (moles of salt/kg of  $\text{D}_2\text{O}$ ) for the systems  $\text{MgCl}_2/\text{D}_2\text{O}$  and  $\text{LiCl}/\text{D}_2\text{O}$ . The temperatures correspond to the stable and metastable, undercooled phase.

TABLE II: Parameters of the Motional Model for the Hydration Waters of the  $\text{Mg}^{2+}$  Cation and the  $\text{Li}^+$  Cation

parameter	$\text{MgCl}_2/\text{D}_2\text{O}$	$\text{LiCl}/\text{D}_2\text{O}$
$\tau_{00}$ , ps	0.170	0.200
$\tau_{10}$ , ps	0.065	0.080
$E_a$ , kJ/mol	21.0 ( $c \leq 4$ m) 21.4 ( $c = 5$ m) <sup>a</sup> 22.0 ( $c = 5$ m) <sup>b</sup>	19.8
$B_r$ , kJ/mol	5.72	5.72
$\chi_{\text{eff}}$ , kHz	192 ( $c \leq 4$ m) 182 ( $c = 5$ m)	192
$n_h$	16 ( $c \leq 3$ m) 12.5 ( $c = 4$ m) 10 ( $c = 5$ m)	6 ( $c \leq 8$ m) 4.55 ( $c = 11$ m)

<sup>a</sup> Tetragonal configuration of hydration waters. <sup>b</sup> Trigonal Configuration of hydration waters.

corresponding to  $\tau_{10} = 65$  fs roughly, has been chosen. The rotational barrier  $E_a$  for orientational fluctuations around the local director has been adjusted with a least-squares fit of the experimental data of the 3 m solution to eq 2. Only the high-field data have been used.

All pertinent model parameters thus obtained are compiled in Table II.

**Calculation of the Relaxation Rate  $R_1(T, R, p = 225 \text{ MPa})$ .** Having determined the hydration water relaxation rate  $(R_1)_{\text{hyd}}$ , the relaxation rate for a solution of composition  $R$  has been calculated within the two-site approximation. However, both rates in eq 6 have to be calculated at the same reduced temperature ( $T = T_0(R)$ ) that corresponds to that of the solution under investigation, because the clusters of hydrated cations and H-bonded bulk water molecules are in dynamic equilibrium.

The dynamic hydration number  $n_h$  was taken to be  $n_h = 16$  for  $R \geq 16$ , thus regarding all water molecules of both hydration shells to be related with the  $\text{Mg}^{2+}$  cations on time scales of the relevant correlation times. In more concentrated solutions  $n_h = R$  was set to account for the decreasing water content of these solutions. All relaxation time isobars  $T_1(T, R, p = 225 \text{ MPa})$ , drawn in Figure 4 as solid lines (except for  $R = 10$ ), have been calculated then with eq 6 without adjusting any further parameter.

In the 5 m solution (close to saturation) most of the molecules belong to the primary hydration shell. These water molecules are strongly polarized and prefer a trigonal orientation on average. Thus the rotational barrier has been estimated with  $\beta_{\text{DF}}$  calculated accordingly (see Table II). To account for the depth of the  $T_1(T)$  curve of the 5 m solution at the minimum, the deuteron quadrupole coupling constant had to be reduced at  $\chi_{\text{eff}} = 182 \text{ kHz}$ . Indicating an increased OD bond length, this result corroborates MD simulations<sup>26</sup> and NMR experiments.<sup>27,28</sup>

## Discussion

**Effect of Pressure and Ionic Solutes upon Molecular Motions.** In liquid water at low temperatures structural correlations develop within the random, transient H-bond network with increasing correlation length and with a strong slowing down of structural fluctuations. These cooperative phenomena become most pronounced close to the low-temperature limit  $T_H$  of the undercooled phase. Dynamic properties of water molecules, related to these structural fluctuations, then display a dynamic scaling behavior according to

$$R_1 \approx \tau \approx (T - T_s)^{-\gamma} \quad (7)$$

with the scaling temperature  $T_s$  a few degrees below  $T_H$ .<sup>2,4</sup> Hydrostatic pressure and/or ionic solutes may be considered network-breaking agents. They suppress long-range structural correlations within the network (hence reduce the correlation length) and shift the low-temperature limit of the undercooled phase (hence also  $T_s$ ) to lower temperatures.<sup>2,6</sup>

Figure 3 shows that  $T_1(T = \text{const})$  increases upon initial compression, indicating that molecular motions become less hindered.  $T_1(T = \text{const})$  also increases upon addition of ionic solutes in the undercooled phase at low pressure. These effects can be easily understood in terms of an increasing distance  $(T - T_s)$  from the scaling temperature  $T_s(c, p)$ , which is a strongly decreasing function of pressure and solute concentration.

Under the combined influence of both network-breaking agents these anomalous effects must become less pronounced.<sup>29</sup> That

(26) Heinzinger, K. *Pure Appl. Chem.* **1985**, 57, 1031.

(27) van der Maarel, J. R. C.; Lankhorst, D.; de Bleijser, J.; Leyte, J. C. *J. Phys. Chem.* **1986**, 90, 1470.

(28) Struis, R. P. W. J.; de Bleijser, J.; Leyte, J. C. *J. Phys. Chem.* **1987**, 91, 1639.

(25) Safford, G. J.; Leung, P. S. *Ber. Bunsen-Ges. Phys. Chem.* **1971**, 75, 366.

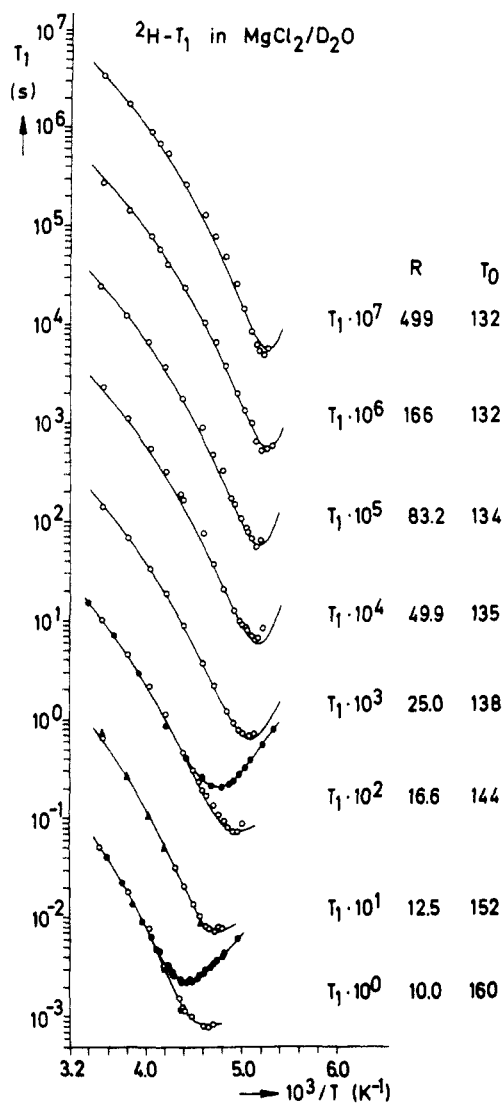


**Figure 4.** Isobaric ( $p = 225$  MPa) temperature dependence of deuteron spin-lattice relaxation times  $T_1$  at various compositions  $R$  (moles of  $D_2O$ /mole of salt): (O)  $\omega_0/2\pi = 15.35$  MHz,  $B_0 = 2.35$  T; (●)  $\omega_0/2\pi = 46.07$  MHz,  $B_0 = 7.05$  T.

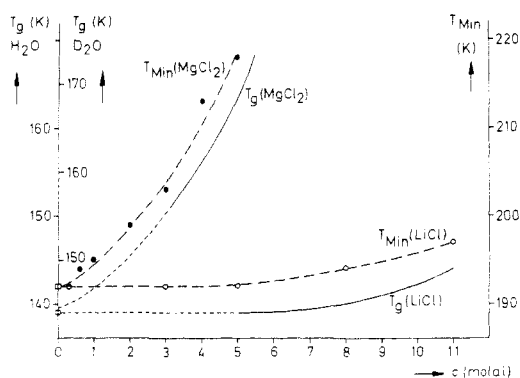


**Figure 5.** Composition dependence of the temperatures  $T_{\min}$  of minimal  $T_1$  compared with experimental glass temperatures  $T_g$  taken from ref 35.

even a solution of composition  $R = 25$  displays the anomalous pressure effect has implications for the average local structures in these systems. Subtracting the cationic hydration water, the correlated H-bonded patches, causing the anomalous pressure effect, can be built up from roughly 10 water molecules at most. Consequently the anions in the solution must be coordinated to the hydrated cations and are not hydrated separately. Hence water

bridging must become important to determine the average local structure in these concentrated solutions.

At the edge of the glass-forming composition range the solutions contain only water molecules hydrating the cations with almost no bulk water present. These molecules are forced into close packing by strong electrostrictive forces. Their average orientation due to ion-dipole forces inhibits optimal H-bond interactions. Hence, the H-bond network is sufficiently disturbed, so that hydrostatic pressure exerts no further influence upon molecular reorientations. Computer simulations indicate that the local structure of the hydration shell is also not changed under hydrostatic pressure.<sup>17</sup>

**Slow Molecular Motions and the Glass Transition.** Dense undercooled liquids often exhibit several characteristic and seemingly universal dynamic properties.<sup>30,31</sup> One of these is a nonexponential relaxation of structural fluctuations emerging either from a hierarchy of relaxation processes or from a superposition of exponentially relaxing processes implying many parallel relaxation paths. There is in fact no way to distinguish both explanations from relaxation experiments alone.

The present motional model represents the most simple example of the latter approach. But, instead of fitting the data to a convenient distribution of correlation times, specific motional modes are considered which are consistent with the local structure in these solutions.<sup>32</sup>

Another characteristic feature is the non-Arrhenius  $T$  dependence of average structural relaxation times. This behavior is clearly visible in Figure 4 and has been ascribed to the tumbling and exchange processes within our two-mode approximation. These modes thus dominate the relaxation at medium undercooling (in the fast motions regime); hence they constitute the primary ( $\alpha$ ) relaxation process.<sup>30</sup> In the slow-motion regime the relaxation rate does not slow down as strongly as is predicted by the VTF law (eq 4). Instead the high-field measurements show a much weaker  $T$  dependence of  $T_1$ . In the current motional model this feature stems from the  $T$  dependence of the localized anisotropic mode. It is considered a thermally activated process with a characteristic Arrhenius behavior. As a consequence the strong slowing down of configurational fluctuations related to the  $\alpha$ -process is not reflected in the  $T_1(T)$  curves. At low temperatures the faster local mode splits off, as a secondary relaxation process,<sup>30</sup> and dominates the relaxation, because it provides the more efficient relaxation channel.

It is instructive to note that in the fast-motion regime the model leads to longer correlation times  $\tau_1$  for the local anisotropic mode compared with the correlation times  $\tau_0$  for overall tumbling and exchange processes. These results are contrary to conclusions drawn from  $^{17}O$  line-width studies in aqueous solutions of diamagnetic metal ions<sup>33</sup> at ambient conditions. The relatively small experimental line widths  $\delta\omega \approx 1/T_2$  have been interpreted in terms of an assumed rapid internal rotation of the water molecules of the hydration complex around the ion-oxygen direction. Because of this rapid rotation part of the quadrupolar interaction of the  $^{17}O$  nucleus would be averaged out, thereby reducing the  $^{17}O$  quadrupole relaxation. Note that within the present model a partial averaging of the pertinent interaction, concomitant with a reduced relaxation, is due to fast torsional oscillations which however contribute nothing to the spectral density function  $g(\omega)$  (see eq 2 and ref 5 and 6). No assumptions about relative time scales of local and overall diffusive modes were necessary in the present treatment.

In this respect it is interesting that the two-step motional model proposed by Halle and Wennerström,<sup>34</sup> who elaborated upon the consequences of a time-scale separation of fast and slow modes

(30) Jäckle, J. *Rep. Prog. Phys.* **1986**, *49*, 171.

(31) Palmer, R. R. In *Heidelberg Colloquium on Glassy Dynamics*; van Hemmen, J. L., Morgenstern, I., Eds.; Springer: Berlin, 1987; Lecture Notes in Physics, Vol. 275, p 275.

(32) Enderby, J. E.; Cummings, S.; Herdman, G. J.; Neilson, G. W.; Salmon, P. S.; Skipper, N. *J. Phys. Chem.* **1987**, *91*, 5851.

(33) Connick, R. E.; Wüthrich, K. *J. Chem. Phys.* **1969**, *51*, 4506.

(34) Halle, B.; Wennerström, H. *J. Chem. Phys.* **1981**, *75*, 1928.

on the relaxation, cannot be made to fit the data if an Arrhenius temperature dependence is appropriate for the fast local mode. This is because in the two-step model the (faster) local mode dominates the relaxation in the fast motions regime ( $T > T_{\min}$ ). Consequently an Arrhenius temperature dependence of  $T_1$  would be expected. Instead the experimental  $T_1$  data show a distinctly non-Arrhenian behavior of the relaxation time curve, which can be represented by a VTF law at high pressures or high solute concentrations where the systems are known to form glasses.<sup>35</sup>

**Acknowledgment.** We are indebted to Prof. Lüdemann for stimulating discussions and critical comments. The technical assistance of H. Knott, S. Heyn, and E. Tremel made this work feasible. Financial support of the DFG and the Fonds der Chemie is gratefully acknowledged.

**Registry No.** MgCl<sub>2</sub>, 7786-30-3.

(35) Angell, C. A.; Sare, E. J. *J. Chem. Phys.* 1970, 52, 1058.

## Comparison of Steady-State Electrical Properties for Two Counterion and Electron-Counterion Membranes

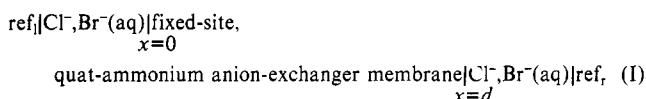
Richard P. Buck

Department of Chemistry, University of North Carolina, Chapel Hill, North Carolina 27599  
(Received: February 17, 1988; In Final Form: April 25, 1988)

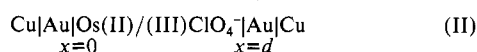
Steady-state electrical properties of fixed-site membranes bathed simultaneously with electrolytes, and contacted by metals, can be treated by both the Nernst-Planck electron-displacement and Saveant electron-hopping equations. Systems with two anions, or anions and electrons, are compared in terms of fields, concentration and voltage profiles, and current-voltage curves. Ohmic and limiting currents at high voltages can occur. Interfacial potentials, ion and electron exchange boundary conditions, and cases of pinned and floating ion electrochemical potentials or Fermi levels are described. Classical Nernst-Planck, ion-exchanging systems with single-charge mobile species are constant field. In contrast, the hopping systems show nearly linear carrier concentration profiles but severely curved fields with absolute maxima where jump sites are in short supply.

### Introduction

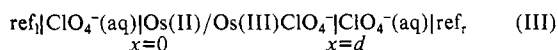
Free-standing, fixed-site membranes, bathed in mixtures of reversibly ion-exchanging counterions are illustrated in a typical ion-contact membrane cell according to



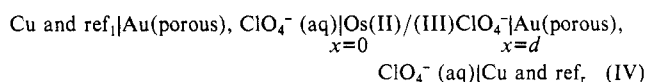
On the other hand, a free-standing, fixed-site mixed-conductor membrane could be contacted with solid, metal electrodes



or with electrolytes

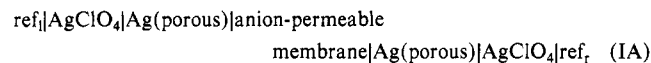


or with metal on one side and electrolyte on the other (combination of II and III), or contacted by porous metals and simultaneously bathed in mixtures of counterions, shown here and illustrated in Figure 1.

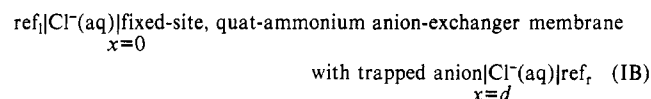


The similarities of cells I-IV become clearer by comparing a synthetic positively charged quaternary ammonium site membrane bathed in mixtures of  $\text{Cl}^-$  and  $\text{Br}^-$  (cell I) with an oxidized, positively charged site polypyrrole membrane bathed in  $\text{Cl}^-$ . The first system contains two mobile counteranions subject to membrane electroneutrality and equality of each ion's electrochemical potential at each interface. The second contains two mobile counter-charged species also: electrons on Red species and a single counteranion. The species Ox is the fixed site.<sup>1</sup>

To relate these cells thermodynamically and conceptually, a mixed-conductor equivalent of cell I is introduced:



Before passing on to cell IV, cells II and III are considered as examples of interfacial blocking. Both are equivalent to a simple ion-exchange membrane cell:



containing some trapped, oil-soluble anion. In cell II, the anion  $\text{ClO}_4^-$  is trapped, while in cell III, the electrons are trapped. Finally, cell IV is treated as anion blocked or electron blocked, depending on the circuit used to apply the voltage (Figure 1).

Transport theory applied to membranes can be used effectively in the steady state because many nonlinear problems are solvable by virtue of the constancy (in time) of concentration profiles, fluxes, and currents. One can deduce from intermediate stages in the analyses whether fields are constant in space, under what voltage conditions individual counterion species contents are conserved in the membranes, whether interfacial pd's are pinned or float by virtue of different applied voltages, and what conditions are present that determine Ohmic or non-Ohmic current-voltage curves. Ultimately one can deduce individual species concentration profiles, fluxes, fields, and currents in terms of independent parameters, usually applied voltages and external solution compositions.

In this paper a step-by-step comparison is made of theoretically similar systems: cell I with two reversibly exchanging counterions in a fixed-site membrane under an applied, external voltage on reversible reference electrodes, compared with cell IV containing an electron and counteranion in a fixed-site membrane contacted by metal and by electrolyte, under applied voltages from reference electrodes. For this analysis of the electron diffusion-migration, simplified Nernst-Planck equations are used for all species because these equations are simply integrable. To reach the cell I/cell IV comparison, two further theoretically similar intermediate systems are analyzed; cell IB with one mobile, reversible anion

(1) Buck, R. P. *J. Electroanal. Chem. Interfacial Electrochem.* 1987, 219, 23-48.